EUROPEAN JOURNAL OF PURE AND APPLIED MATHEMATICS
2025, Vol. 18, Issue 3, Article Number 6203
ISSN 1307-5543 – ejpam.com
Published by New York Business Global

Mathematical Modeling and Analysis of Immobilized Glucose Dehydrogenase Glucose and Oxygen-Driven Reactions in Spherical Micro-reactors

Daniel S[1,2], Mallikarjuna M[1,3], Senthamarai R[1,*]

[1] *Department of Mathematics, College of Engineering and Technology, SRM Institute of Science and Technology, Kattankulathur – 603 203, Tamilnadu, India*
[2] *PG & Research Department of Mathematics, Cardamom Planters' Association College, Bodinayakanur-625 582, Tamil Nadu, India*
[3] *Department of Mathematics, Karpaga Vinayaga College of Engineering and Technology, Madhuranthagam, Tamil Nadu 603308, India*

Abstract. In this article, a batch stirred tank reactor comprising an array of uniform spherical porous micro-reactor (MR) immobilized with nonspecific glucose dehydrogenase and an oxygen-reducing enzyme is modeled mathematically. This model is a steady-state system of non-linear reaction diffusion terms related to the non-Michaelis-Menten kinetics of an enzymatic reaction. We provide approximate analytical expression of the non-linear reaction diffusion equations of substrate, product and oxygen concentrations by utilizing the Adomian Decomposition Method (ADM) and Taylor Series Method (TSM). The obtained semi-analytical results are compared with the numerical simulations, satisfactory results are obtained. Semi-analytical expression for the effectiveness factor of the system is also provided. Using this expression, the factors influencing the effective operation of the system are discussed.

2020 Mathematics Subject Classifications: 34A34, 34A45, 34B15, 34B60, 92C45

Key Words and Phrases: Micro-reactor, Analytical solution, Taylor series Method, Adomian Decomposition Method, Adomian polynomials

1. Introduction

Micro-reactors (MR) with immobilized enzymes enable selective substrate conversions, efficient utilization of small sample and reagent volumes, cost reduction, shorter process times, and a compact system design [1, 2]. Enzyme immobilization may lead to some loss of activity; however, it often enhances stability by confining the enzyme within support materials [3, 4]. For the process of integration of a micro-reactor into a stirred tank reactor,

*Corresponding author.
DOI: https://doi.org/10.29020/nybg.ejpam.v18i3.6203

Email addresses: daniel.s@cpacollege.org (Daniel S),
mallikarjuna363@gmail.com (M. Mallikarjuna) senthamr@srmist.edu.in (Senthamarai R)

the support material must withstand shear forces [5]. Porous silica-based materials serve as excellent supports due to their tunable properties, enabling high enzyme loading [1, 6, 7].

The development and enhancement of highly efficient and productive biological processes require the assessment and consideration of various physical and biochemical characteristics [1, 8]. In numerous bioreactors, both liquid and solid phases coexist, making mass transfer a crucial factor to consider [8, 9]. Pore and particle size play a crucial role in determining the total surface area, directly influencing enzyme binding capacity [10]. One approach to optimizing micro-reactor characteristics is through extensive physical experimentation. Alternatively, advanced computational modeling techniques can be employed to simulate and analyze bioreactor processes for further improvement [11].

Recently, various mathematical models representing the batch reactors have been created. Sánchez et al. [12] compared the continuous-flow activated sludge and sequencing batch reactor processes using math to see how well they remove carbon and nitrogen while looking at different operating conditions. Rivera et al. [13] studied the use of computational fluid dynamics (CFD) for modeling electrochemical reactors to enhance the existing technologies and develop new applications. It highlights CDF-driven optimizations in reactor design, electrode configuration, fluid distribution, and operational conditions for various industrial and environmental processes. Harker et al. [14] presented a deterministic method for calculating key parameters (k_2, k_3) in anaerobic digestion (AD) using the AM2 model, with a focus on volatile fatty acid concentration dynamics. Their approach demonstrated high accuracy, with global error below 2.37%, ensuring reliable parameter estimation.

Obtaining an analytical solution for a non-linear differential equation is the constant problem faced by the researchers. Various iterative methods have been utilized recently for obtaining the semi-analytical solutions for the non-linear differential equations, which can be utilized for better understanding of the physical system. Mallikarjuna and Senthamarai [15] utilized the TSM and ADM for obtaining the semi-analytical solutions of non-linear differential equations of substrate and product concentrations arising in amperometric biosensors in steady-state conditions, and for non-steady-state conditions, they utilized the Laplace homotopy perturbation method [16]. Recently, they also utilized the ADM for analyzing the steady-state non-linear model of the batch reactor performance for the synthesis of cephalexin [17]. Sivakumar et al. [18, 19] provided the semi-analytical expressions for the non-steady-state immobilized enzyme systems with and without the external mass transfer resistance by utilizing the Laplace homotopy perturbation method. WM Al-Hayani [20] presented the combination of the Laplace transform and the homotopy perturbation method for solving the sine-Gordon equation.

The variational iteration method was utilized by Senthamarai and Saibhavani [21] for providing the semi-analytical solution for the non-linear differential equation arising in the immobilized enzyme reactor. WM Al-Hayani and MT Younis [22] provided an ap-

proximate analytical method for Green's function by utilizing the homotopy perturbation method. They also provided an approximate analytical solution for the linear and non-linear parabolic and hyperbolic partial differential equations using the same methodology [23]. El-Ajou et al. [24] introduced the Laplace Residual Power series method to obtain analytical solutions for various ordinary differential equations, including singular, non-singular, linear, and non-linear cases. Olayiwola et al. [25] developed a mathematical model to evaluate the impact of antiviral drugs and monoclonal antibodies on COVID-19 transmission, analyzing stability, sensitivity, and solution uniqueness using the Laplace-ADM and real-world data. Awonusika [26] applied the ADM to obtain analytical solutions for a class of Lane-Emden equations involving Jacobi functions, presenting power series and closed-form solutions for specific cases. Comparisons with existing results confirm the method's accuracy and reliability in solving these equations across various symmetric and hyperbolic spaces. Mahmood et al. [27] applied the ADM for weakly non-linear systems of harmonic oscillators with separate resonance passages. Waleed Al-Hayani [28] utilized the combination of ADM with the Green's function for solving the linear and non-linear boundary value problem of twelfth order. Usman et al. [29] utilized the Natural transform and ADM for solving the 2-dimensional heat equation which is a non-homogeneous PDE. Silambuselvi et al. [30] studied the mathematical model of facilitated diffusion process in liquid membrane by utilizing the ADM. They provided semi analytical results for the solute, ligand and solute ligand complex and for the facilitator factor of the system. Mebarek et al. [31] utilized the ADM for solving the non-linear differential equations representing the boron diffusion during the boronizing process.

To the best of the authors' knowledge, no semi-analytical solution currently exists for the mathematical model of a microreactor incorporating glucose dehydrogenase and laccase enzymes immobilized within carbon nanotubes under steady-state conditions. This study aims to bridge that gap by providing a comprehensive analysis of the system, offering valuable insights into the optimization of enzyme-based micro-reactors.

In this research article, a mathematical model of a micro-reactor with the bienzyme system of glucose dehydrogenase and lactase immobilized into the carbon nanotubes is analyzed. The major contribution of this research is that the non-linear term in the reaction-diffusion equation is based on the non-Michaelis-Menten type enzymatic kinetics. The semi-analytical expression for the non-linear reaction diffusion equation is obtained by utilizing the TSM and ADM. Obtained analytical results are compared with the numerical simulation, and it is seen that the results correlate satisfactorily for all the values of parameters appearing in the system. The analytical expression for the effective working of the micro-reactor is also obtained and vanished. The effect of parameters on the concentrations and effective working of the system are analyzed by utilizing the obtained analytical results.

This research helps to understand the theoretical and practical optimization of the bioenzyme systems immobilized on the carbon nanotubes. The semi-analytical solutions

obtained by utilizing the ADM and TSM offer a valuable tool for predicting substrate and product concentrations under varying parametric conditions, which is helpful in optimizing the micro-reactor. These findings have a broad range of applications in biomedical engineering for developing more enhanced biosensors and bioreactors, pharmaceuticals for drug synthesis using enzymes, and wastewater treatment. This study provides a strong analytical foundation for improvising enzyme-based reaction systems in diverse biotechnological applications.

This research work is articulated as in Section 2, the mathematical model is given; in Section 3, the semi-analytical solution of the non-linear reaction diffusion equation is depicted; Section 4 depicts the validation of the analytical results; Section 5 depicts the major results of the article; and the conclusion is given in Section 6.

2. Mathematical Formulation of the Problem

The subsequent biochemical reactions that occur in the micro-reactor are taken into account for the modelling. Assuming all the following equations satisfy the Michaelis–Menten kinetics.

$$L + E_{1OX} \xrightarrow{k_1} P + E_{1red}, \tag{1}$$

$$E_{1red} \xrightarrow{k_2} E_{1OX} + 2e^-, \tag{2}$$

$$E_{2OX} + 4e^- \xrightarrow{k_3} E_{2red}, \tag{3}$$

$$E_{2red} + O_2 \xrightarrow{k_4} E_{2OX} + 2H_2O, \tag{4}$$

where L, O_2, and H_2O denote lactose, oxygen, and water. The oxidized and reduced enzymes for GDH are E_{1OX} and E_{1red}, E_{2red} stands for lactose, and P is the reaction product. Also, k_1 and k_4 stand for rate reaction constants of enzyme reactions, and k_2 and k_3 stand for rate reaction constants of enzyme transfer.

Outside of the MR, no enzymatic or energy transfer reactions occur. The Nernst diffusion layer, a thin spherical shell adjacent to the MR surface, remains stagnant over time, assuming that the solution is constantly stirred and the Nernst approach is applied. Therefore, only the mass transport by diffusion occurs in the shell that encircles the MR. When the solution is outside the diffusion shell, it is moving, and the amounts of all the soluble substances are the same all around outside the shell. The schematic representation of immobilized glucose spherical micro-reactor is represented in Fig. 1.

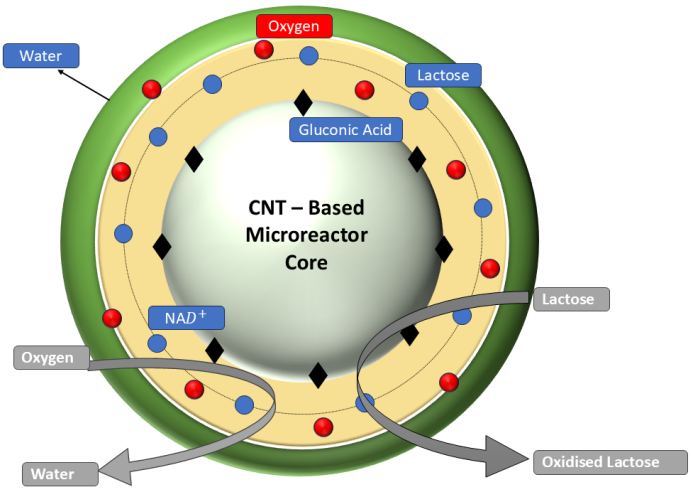

Figure 1: Schematic representation of immobilized glucose spherical micro-reactor

Nomenclature

Symbol	Meaning
L_m	Concentration of Lactose
P_m	Concentration of Product
O_m	Concentration of Oxygen
$L_b,\ P_b,\ O_b$	Bulk concentrations
r	Spherical Co-ordinate
R	Thickness of Spherical Co-ordinate
$V_L,\ V_O$	Volumetric Reaction Rate
$K_L,\ K_O$	Michaelis-Menten Constants
A	Dimensionless Concentration of Lactose
C	Dimensionless Concentration of Product
B	Dimensionless Concentration of Oxygen
χ	Dimensionless Spherical Co-ordinate
$\phi_1^2,\ \phi_2^2,\ \phi_3^2$	Dimensionless Diffusion Parameters
$\alpha,\ \beta,\ \gamma,\ \sigma$	Dimensionless Saturation Parameters
η	Effectiveness Factor
ADM	Adomian Decomposition Method
TSM	Taylor Series Method
MR	Micro-Reactor
EF	Effectiveness Factor

Based on the reaction inside and outside the MR, the steady-state mathematical model is formed. L_m, P_m, O_m represents the concentration of lactose, product, and oxygen, respectively.

The following are the dimensional steady-state differential equations [11]

$$D_{l,m}\left(\frac{d^2L_m}{dr^2}+\frac{2}{r}\frac{dL_m}{dr}\right)=V, \tag{5}$$

$$D_{p,m}\left(\frac{d^2P_m}{dr^2}+\frac{2}{r}\frac{dP_m}{dr}\right)=-V, \tag{6}$$

$$D_{o,m}\left(\frac{d^2O_m}{dr^2}+\frac{2}{r}\frac{dO_m}{dr}\right)=\frac{V}{2}, \tag{7}$$

where $P_m(r)$ depicts the product concentration of the MR, $L_m(r)$ and $O_m(r)$ are the volumetric concentrations of the lactose and oxygen, respectively, and r is the spherical coordinate of the MR,
where

$$V=\frac{2V_LV_OL_mO_m}{K_OL_mV_L+2K_LO_mV_O+L_mO_mV_L+2L_mO_mV_O}, \tag{8}$$

due to the symmetry zero-flux boundary conditions are defined on the center of the MR

$$D_{S,m}\frac{dS_m}{dr}\bigg|_{r=0}=0, \quad S=L,\ P,\ O. \tag{9}$$

On the boundary between the diffusion and convective shells ($r=R_1$), the continuity of the concentrations is required

$$S_d(R_1)=S_b, \quad S=L,\ P,\ O, \tag{10}$$

for the ease of the solution we utilize the following non-dimensional parameters for non-dimensionalizing the governing equations:

$$\begin{gathered}A(\chi)=\tfrac{L_m}{L_b},\ B(\chi)=\tfrac{O_m}{O_b},\ C(\chi)=\tfrac{P_m}{P_b},\ \chi=\tfrac{r}{R_1},\\ \phi_1^2=\tfrac{R^2V_LV_0}{D_{l,m}},\ \phi_2^2=\tfrac{R^2V_LV_0}{D_{p,m}},\ \phi_3^2=\tfrac{R^2V_LV_0}{D_{o,m}},\\ \alpha=V_LK_OL_b,\ \beta=O_bK_LV_O,\ \gamma=O_bL_bV_L,\ \sigma=V_OL_bO_b,\end{gathered} \tag{11}$$

the non-dimensional governing equation for the lactose, product and oxygen concentrations is obtained as follows:

$$\frac{d^2A(\chi)}{d\chi^2}+\frac{2}{\chi}\frac{dA(\chi)}{d\chi}=\phi_1^2\frac{2A(\chi)B(\chi)}{\alpha A(\chi)+2\beta B(\chi)+\gamma A(\chi)B(\chi)+2\sigma A(\chi)B(\chi)}, \tag{12}$$

$$\frac{d^2C(\chi)}{d\chi^2}+\frac{2}{\chi}\frac{dC(\chi)}{d\chi}=-\phi_2^2\frac{2A(\chi)B(\chi)}{\alpha A(\chi)+2\beta B(\chi)+\gamma A(\chi)B(\chi)+2\sigma A(\chi)B(\chi)}, \tag{13}$$

$$\frac{d^2B(\chi)}{d\chi^2}+\frac{2}{\chi}\frac{dB(\chi)}{d\chi}=\phi_3^2\frac{A(\chi)B(\chi)}{\alpha A(\chi)+2\beta B(\chi)+\gamma A(\chi)B(\chi)+2\sigma A(\chi)B(\chi)}, \tag{14}$$

with boundary conditions,
when $\chi = 0$,

$$\left.\frac{dN}{d\chi}\right|_{\chi=0} = 0, \quad N = A,\ C,\ B, \tag{15}$$

when $\chi = 1$,

$$N(1) = 1, \quad N = A,\ C,\ B, \tag{16}$$

The effectiveness factor of the system is given as

$$\eta = \frac{3(\alpha+\beta+\gamma+\sigma)}{2\phi_2^2}\left.\frac{dC}{d\chi}\right|_{\chi=1}, \tag{17}$$

3. Semi-Analytical Expressions of Concentration of Lactose, Product and Oxygen

Finding an exact solution to a non-linear differential equation is highly challenging. Solving a system of non-linear differential equations remains one of the most complex problems faced by researchers today.

In this paper we use two different methods to solve the non-linear equations, the first one was Taylor's series is an infinite accumulation of terms that are expressed on a single point in terms of the derivatives of a function. Without the use of linearization, perturbation, or transformation, the analytical solution is generated by the TSM in the form of highly convergent infinite power series with instantly computable terms.

The second method we used is the ADM. It was primarily done by George Adomian in the 1980s [32–34]. It generates results without requiring linearization, perturbation, or discretization of the system. It maintains the accuracy of numerical solutions while significantly reducing computational effort.

3.1. Semi-analytical expressions utilizing Taylor Series Method

We use the TSM (see Appendix A) to obtain the semi-analytical solution for the governing Eqs. (12) - (16).

Solving the Eqs. (12) - (14) for boundary conditions (15) and (16), we get

$$
\begin{aligned}
A(\chi) &= 1 + l(\chi-1) + \frac{(\chi-1)^2}{2!}\left(-2l + \frac{2\phi_1^2}{\alpha+2\beta+\gamma+2\sigma}\right) \\
&+ \frac{(\chi-1)^3}{3!(\alpha+2\beta+\gamma+2\sigma)^2}\left(\begin{array}{l}\left(6\alpha^2+(24\beta+12\gamma+24\sigma)\alpha+24\beta^2+(4\phi_1^2+24\gamma+48\sigma)\beta\right.\\ \left.+6(\gamma+2\sigma)^2\right)l+2\phi_1^2\left((n-2)\alpha-4\beta-2\gamma-4\sigma\right)\end{array}\right) \\
&+ \frac{(\chi-1)^4}{4!(\alpha+2\beta+\gamma+2\sigma)^3}\left(\begin{array}{l}-8(\gamma+2\sigma+\alpha)\beta\phi_1^2l^2+\left(16\beta\left((n-1)\alpha-2\beta-\gamma-2\sigma\right)\phi_1^2\right.\\ \left.-192\left(\frac{\gamma}{2}+\sigma+\frac{\alpha}{2}+\beta\right)^3\right)l-8\phi_1^2\left(-\beta\phi_1^2+(n-2)\alpha^2+\right.\\ \left.\left((n^2+2n-8)\beta+\left(\frac{n^2}{2}+n-4\right)\gamma+(n^2+2n-8)\sigma-\frac{\phi_3^2}{4}\right)\alpha\right.\\ \left.-8\left(\frac{\gamma}{2}+\sigma+\beta\right)^2\right)\end{array}\right) \\
&+ \frac{(\chi-1)^5}{5!(\alpha+2\beta+\gamma+2\sigma)^4}\left(\begin{array}{l}16\beta\left(\left(-3l+\frac{7n}{2}-2\right)\alpha+(l-4)\beta-3\left(l+\frac{2}{3}\right)(\gamma+2\sigma)\right)\phi_1^4\\ +\left((40n-80)\alpha^3+\left((24l^3+(-48n+64)l^2+(24n^2-128n\right.\right.\\ \left.+80)l+64n^2+160n-480)\beta+(32n^2+80n-240)\gamma\right.\\ \left.+(64n^2+160n-480)\sigma+2\phi_3^2(n-4)\right)\alpha^2+\left(((48n+128)l^2\right.\\ \left.+(-96n^2-256n+320)l+48n^3+128n^2+160n-960)\beta^2\right.\\ +\left(\left((48\gamma+96\sigma)l^3-48(n-\frac{8}{3})(\gamma+2\sigma)l^2+\left((-48n^2-128n\right.\right.\right.\\ \left.\left.+160)\gamma+(-96n^2-256n+320)\sigma+28\phi_3^2\right)l+(48n^3+128n^2\\ \left.+160n-960)\gamma+(96n^3+256n^2+320n-1920)\sigma\right.\\ \left.-24\phi_3^2(n+\frac{2}{3})\right)\beta+12\left(\left(n^3+\frac{8}{3}n^2+\frac{10}{3}n-20\right)\gamma\right.\\ \left.+\left(2n^3+\frac{16}{3}n^2+\frac{20}{3}n-40\right)\sigma-\phi_3^2(n+\frac{2}{3})\right)(\gamma+2\sigma)\Big)\alpha\\ +(320l-640)\beta^3+128\left(l^2+\frac{5}{2}l-\frac{15}{2}\right)(\gamma+2\sigma)\beta^2\\ +24(l^3+\frac{8}{3}l^2+\frac{10}{3}l-20)(\gamma+2\sigma)^2\beta-80(\gamma+2\sigma)^3\Big)\phi_1^2\\ +1920\left(\frac{\gamma}{2}+\sigma+\frac{\alpha}{2}+\beta\right)^4l\end{array}\right)
\end{aligned}
\tag{18}
$$

$$
\begin{aligned}
C(\chi) &= 1 + m(\chi-1) - \frac{(\chi-1)^2}{2!}\left(2m + \frac{2\phi_2^2}{\alpha+2\beta+\gamma+2\sigma}\right) \\
&+ \frac{(\chi-1)^3}{3!(\alpha+2\beta+\gamma+2\sigma)^2}\left(24\left(\frac{\gamma}{2}+\sigma+\frac{\alpha}{2}+\beta\right)^2 m - 4\left(\frac{n}{2}-1\right)\alpha + (l-2)\beta - \gamma - 2\sigma)\phi_2^2\right) \\
&+ \frac{(\chi-1)^4}{4!(\alpha+2\beta+\gamma+2\sigma)^3}\left(\begin{array}{l}
\big((8n-16)\alpha^2 + ((8l^2+(-16n+16)l+8n^2+16n-64)\beta \\
+(4n^2+8n-32)\gamma + (8n^2+16n-64)\sigma - 2\phi_3^2)\alpha \\
+(32l-64)\beta^2 + ((8l^2+16l-64)\gamma + (16l^2+32l-128)\sigma \\
-8\phi_1^2)\beta - 16(\gamma+2\sigma)^2\big)\,\phi_2^2 - 192\left(\frac{\gamma}{2}+\sigma+\frac{\alpha}{2}+\beta\right)^3 m
\end{array}\right) \\
&+ \frac{(\chi-1)^5}{5!(\alpha+2\beta+\gamma+2\sigma)^4}\left(\begin{array}{l}
\big((-40n+80)\alpha^3 + (\big(-24l^3+(48n-64)l^2+(-24n^2+128n \\
-80)l - 64n^2 - 160n + 480\big)\,\beta + (-32n^2-80n+240)\gamma \\
+(-64n^2-160n+480)\sigma - 2\phi_3^2(n-4))\alpha^2 + \big(((-48n-128)l^2 \\
+(96n^2+256n-320)l - 48n^3 - 128n^2 - 160n + 960)\beta^2 \\
+((-48l^3+(48n-128)l^2+(48n^2+128n-160)l - 48n^3 \\
-128n^2 - 160n + 960)\gamma + (-96l^3+(96n-256)l^2 \\
+(96n^2+256n-320)l - 96n^3 - 256n^2 - 320n + 1920)\sigma \\
+(48\phi_1^2 - 28\phi_3^2)l + (-56\phi_1^2 + 24\phi_3^2)n + 16\phi_3^2 + 32\phi_1^2)\beta \\
+12\left(\left(-n^3 - \frac{8}{3}n^2 - \frac{10}{3}n + 20\right)\gamma + (-2n^3 - \frac{16}{3}n^2 - \frac{20}{3}n \right. \\
\left. +40)\sigma + \phi_3^2(n+\frac{2}{3})\right)(\gamma+2\sigma)\Big)\alpha + (-320l+640)\beta^3 \\
+((-128l^2-320l+960)\gamma + (-256l^2-640l+1920)\sigma \\
-16\phi_1^2(l-4))\beta^2 - 24\left(\left(l^3+\frac{8}{3}l^2+\frac{10}{3}l-20\right)\gamma \right. \\
\left. + \left(2l^3+\frac{16}{3}l^2+\frac{20}{3}l-40\right)\sigma - 2(l+\frac{2}{3})\phi_1^2\right)(\gamma+2\sigma)\beta \\
+80(\gamma+2\sigma)^3\big)\,\phi_2^2 + 1920\left(\frac{\gamma}{2}+\sigma+\frac{\alpha}{2}+\beta\right)^4 m
\end{array}\right)
\end{aligned}
\tag{19}
$$

$$
\begin{aligned}
B(\chi) &= 1 + n(\chi-1) + \frac{(\chi-1)^2}{2!}\left(-2n + \frac{\phi_3^2}{\alpha+2\beta+\gamma+2\sigma}\right) \\
&+ \frac{(\chi-1)^3}{3!(\alpha+2\beta+\gamma+2\sigma)^2}\left(6\alpha^2 + (\phi_3^2+24\beta+12\gamma+24\sigma)\alpha + 24(\beta+\frac{\gamma}{2}+\sigma)^2)n + 2\phi_3^2(-\alpha+(l-2)\beta-\gamma-2\sigma)\right) \\
&+ \frac{(\chi-1)^4}{4!(\alpha+2\beta+\gamma+2\sigma)^3}\left(\begin{array}{l} -4\alpha\phi_3^2(\beta+\frac{\gamma}{2}+\sigma)n^2 + (8(-\frac{\alpha}{2}+(l-1)\beta-\frac{\gamma}{2}-\sigma)\alpha\phi_3^2 - \\ 192(\frac{\gamma}{2}+\sigma+\frac{\alpha}{2}+\beta)^3)n - 4\phi_3^2\left(-\frac{\alpha\phi_3^2}{4} - 2\alpha^2\right. \\ +((l^2+2l-8)\beta-4\gamma-8\sigma)\alpha + (4l-8)\beta^2 + ((l^2+2l-8)\gamma \\ +(2l^2+4l-16)\sigma - \phi_1^2)\beta - 2(\gamma+2\sigma)^2) \end{array}\right) \\
&+ \frac{(\chi-1)^5}{5!(\alpha+2\beta+\gamma+2\sigma)^4}\left(\begin{array}{l} 14\left(\left(\frac{n}{14}-\frac{2}{7}\right)\alpha + \left(l-\frac{6n}{7}-\frac{4}{7}\right)\beta - \frac{3(n+\frac{2}{3})(\gamma+2\sigma)}{7}\right)\alpha\phi_3^4 \\ +\left((20n-40)\alpha^3 + \left(((12l+32)n^2 + (-24l^2-64l+80)n + \right.\right. \\ \left.\left.12l^3+32l^2+40l-240)\beta + 16(n^2+\frac{5}{2}n-\frac{15}{2})(\gamma+2\sigma)\right)\alpha^2\right. \\ +\left(\left(24n^3+(-48l+64)n^2+(24l^2-128l+80)n+64l^2+160l\right.\right. \\ \left.\left.-480\right)\beta^2 + \left((24\gamma+48\sigma)n^3 - 24(\gamma+2\sigma)(l-\frac{8}{3})n^2 + ((-24l^2\right.\right. \\ \left.\left.-64l+80)\gamma + (-48l^2-128l+160)\sigma + 28\phi_1^2)n + (24l^3+64l^2\right. \\ \left.+80l-480)\gamma + (48l^3+128l^2+160l-960)\sigma - 24\phi_1^2\left(l+\frac{2}{3}\right)\right)\beta \\ +6(n^3+\frac{8}{3}n^2+\frac{10}{3}n-20)(\gamma+2\sigma)^2\Big)\alpha + (160l-320)\beta^3 \\ +\left((64l^2+160l-480)\gamma + (128l^2+320l-960)\sigma\right. \\ \left.+8\phi_1^2(l-4)\right)\beta^2 + 12(\gamma+2\sigma)\left((l^3+\frac{8}{3}l^2+\frac{10}{3}l-20)\gamma\right. \\ +(2l^3+\frac{16}{3}l^2+\frac{20}{3}l-40)\sigma - 2\phi_1^2(l+\frac{2}{3})\Big)\beta - 40(\gamma+2\sigma)^3\Big)\phi_3^2 \\ +1920\left(\frac{\gamma}{2}+\sigma+\frac{\alpha}{2}+\beta\right)^4 n \end{array}\right)
\end{aligned}
\tag{20}
$$

The constants l, m, n can be determined from Eqs. (18) - (20) for different values of the parameters α, β, γ, σ ϕ_1^2, ϕ_2^2 and ϕ_3^2.
The effectiveness factor is obtained as

$$\eta = \frac{3\left(\alpha+\beta+\gamma+\sigma\right)}{2\phi_2^2}\left(1+l\right), \tag{21}$$

3.2. Semi-analytical expressions utilizing Adomian Decomposition Method

We use the ADM (See Appendix B) to obtain the semi-analytical solution for the governing Eqs. (12) - (16).

We obtain a solution for $A(\chi), C(\chi)$ and $B(\chi)$

$$A(\chi) = 1 + \frac{\phi_1^2(\chi^2-1)}{3(\alpha+2\beta+\gamma+2\sigma)} + \frac{\phi_1^2(\alpha\phi_3^2+4\beta\phi_1^2)}{6(\alpha+2\beta+\gamma+2\sigma)^3}\left(\frac{\chi^4}{20}-\frac{\chi^2}{6}+\frac{7}{60}\right), \tag{22}$$

$$C(\chi) = 1 + \frac{\phi_2^2(1-\chi^2)}{3(\alpha+2\beta+\gamma+2\sigma)} + \frac{\phi_2^2(\alpha\phi_3^2+4\beta\phi_1^2)}{6(\alpha+2\beta+\gamma+2\sigma)^3}\left(\frac{\chi^4}{20}-\frac{\chi^2}{6}-\frac{7}{60}\right), \tag{23}$$

$$B(\chi) = 1 + \frac{\phi_3^2(\chi^2-1)}{6(\alpha+2\beta+\gamma+2\sigma)} + \frac{\phi_3^2(\alpha\phi_3^2+4\beta\phi_1^2)}{12(\alpha+2\beta+\gamma+2\sigma)^3}\left(\frac{\chi^4}{20}-\frac{\chi^2}{6}+\frac{7}{60}\right), \tag{24}$$

effectiveness factor of the system is obtained as

$$\eta = \frac{3\left(\alpha+\beta+\gamma+\sigma\right)}{2\phi_2^2}\left(-\frac{2\phi_2^2}{3\alpha+3\beta+3\gamma+3\sigma} - \frac{\phi_2^2\left(\alpha\phi_3^2+4\beta\phi_1^2\right)}{45\left(\alpha+2\beta+\gamma+2\sigma\right)^3}\right). \tag{25}$$

4. Validation of Analytical Results

The governing system of non-linear differential Eqs. (12) - (14) have been solved analytically by utilizing the semi-analytical methods, the TSM for the Eqs. (18) - (20) and the ADM for the (22) - (24). The numerical simulation of the governing equations has been carried out by utilizing the MATLAB software. The analytical results are compared with the simulated numerical results to obtain satisfactory results. Figs. 2 - 4 represents the comparison between the numerical, TSM, and ADM; it is observed from the graphs that numerical and analytical results correlate satisfactorily. Tables 1 - 3 present the relative error between the numerical, TSM, and ADM. The maximum deviation between the numerical and TSM is 0.063%, while the ADM shows a maximum discrepancy of 0.122%.

In contrast to the previous work by Baronas et al. [11], where the numerical method is directly applied to the system without transformation, this study introduces a non-dimensionalized mathematical model. This enhances generalizability and allows systematic analysis of key parameters such as diffusion and saturation. Additionally, the semi-analytical methods provide explicit closed-form expressions that provide improved interpretability of system behaviors under varying parametric conditions. The dual approach of utilizing both ADM and TSM offers an analytical depth and feasibility not explored in the earlier studies. The comparative analysis against numerical results confirms both the accuracy and reliability of the semi-analytical approaches. The results not only validate the methods but also demonstrate their applicability for optimizing reactor design and for understanding the influence of parameters on the system more comprehensively than traditional numerical methods alone. The analytical framework can be extended to similar multi-enzyme systems, offering a general modeling approach for a class of biocatalytic micro-reactors.

5. Result and Discussion

Figs. 2 - 4 represent the concentration profiles of lactose, product and oxygen in the MR. It is observed that these concentrations depend on the diffusion parameters $\phi_i^2,\ i = 1, 2, 3$, saturation parameters $\alpha,\ \beta,\ \gamma,$ and σ, and the dimensionless distance χ.

5.1. Effect of catalyzed enzyme space

The dimensionless distance within the immobilized MR has a major effect on the concentrations and the effective working of the batch reactor. From Figs. 2a - 2d, it can be seen that the increase in dimensionless distance increases the concentration of lactose in the MR and attains its maximum when $\chi = 1$. Figs. 3a - 3d represent the dimensionless concentration of product in the MR. We can see that the dimensionless distance has the inverse effect as it increases, the concentration decreases and attains zero when $\chi = 1$. Figs. 4a - 4d depict the concentration of oxygen; it is observed that as the enzymatic reaction takes place, the oxygen is released from the enzyme-immobilized MR. From these figures it is observed that the oxygen increases with the increase of the dimensionless distance.

5.2. Effect of saturation parameters

The relationships between bulk concentrations and the kinetic parameters are represented as α, β, γ, and σ. These parameters characterize the extent to which the catalytic kinetics exhibit saturation ($n > 1,$ where $n = \alpha,\ \beta,\ \gamma,\ \sigma$) or remain unsaturated ($n < 1$). Figs. 2, 3 and 4 represent the effect of the saturation parameters on the concentrations of lactose, product, and oxygen. From these figures it is observed that the increase in parameter increases the concentration of lactose and oxygen but has an inverse effect on the concentration of product, as the increase in parameter decreases the concentration of product. We can see that the concentration becomes uniform when $\alpha \geq 100$ for lactose, product, and oxygen. The same is observed for the rest of the parameters β, γ, and σ.

5.3. Effect of the diffusion module

The diffusion module $\phi_i,\ i = 1, 2, 3$ quantifies the relation between the maximum reaction rates of lactose and oxygen to the rate of the diffusion through the MR. Table. 1 - 3 represents the effect of the diffusion module on the concentrations of lactose, product, and oxygen. From the Tables. 1 - 3 we can see that the decrease in the values of diffusion parameters ϕ_1 and ϕ_3 decreases the concentration of lactose and oxygen. But in the case of product concentration, the diffusion module ϕ_2^2 has the inverse effect: as the values increase, it decreases the concentration of product.

5.4. Effectiveness factor of the system

The effectiveness factor (EF) denotes the ratio of the reaction rate inside the pellet to the reaction rate at its outer surface. Its dimensionless metric ranges from 1.8 to 2, serving

as the measure for the catalytic efficiency. The effectiveness factor measures the actual reaction rate within the immobilized pellet relative to the reaction rate in the absence of diffusion limitations. When the entire pellet volume reacts at a high rate, η approaches 2, whereas it nears its minimum value when the reaction within the pellet occurs at a slower rate. The semi-analytical expressions of the effectiveness factor of the MR are obtained using the TSM and ADM. From the Figs. 5a - 5d represents the influence of the diffusion modulus ϕ_2^2 and saturation parameters on the effectiveness factor of the system. It is observed from the figures that saturation parameters are increasing functions; as their values increase, the effectiveness factor of the system also increases. The increase in diffusion modulus ϕ_2^2 decreases the effectiveness of the MR with carbon nanotubes.

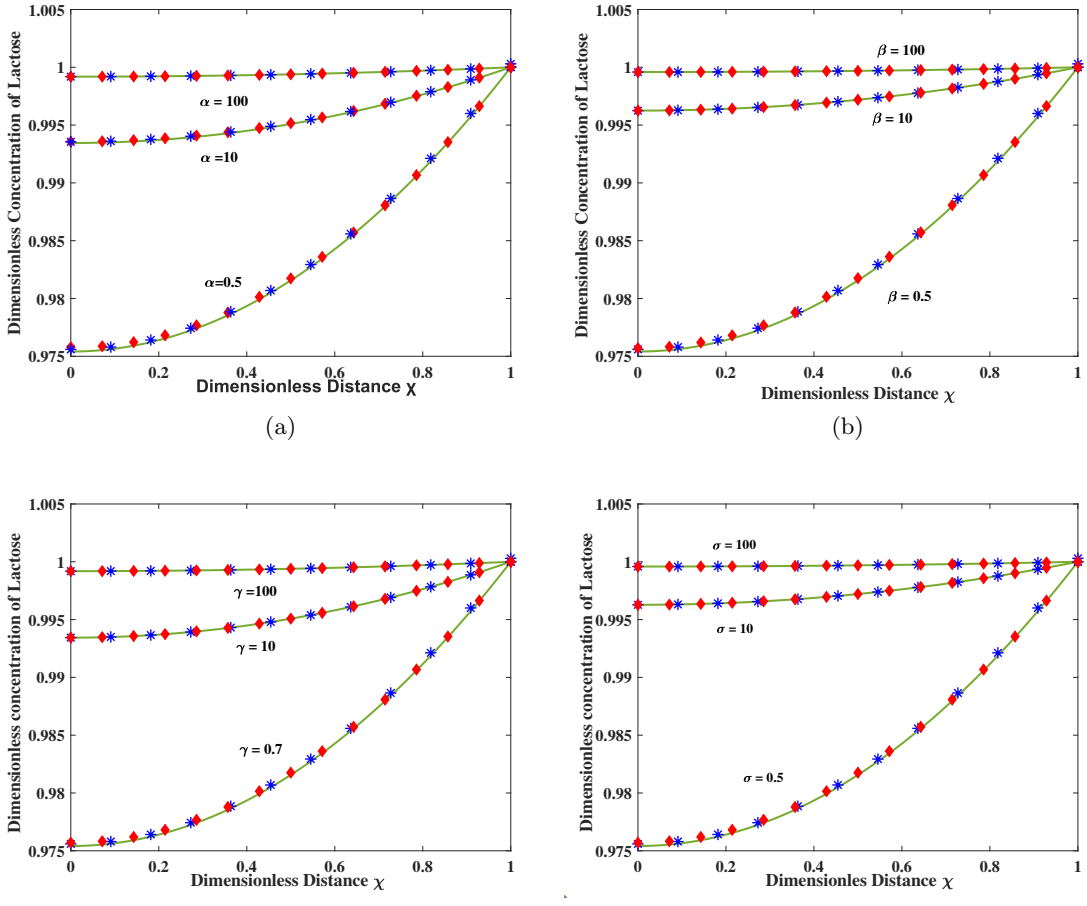

Figure 2: Dimensionless concentration for Lactose $A(\chi)$ versus the dimensionless distance χ for various values of the parameters (2a) α, (2b) β, (2c) γ, (2d) σ where '$\cdots$' denotes the numerical solution, '***' represents the ADM solution, and '$\diamond\diamond\diamond$' corresponds to the TSM solution.

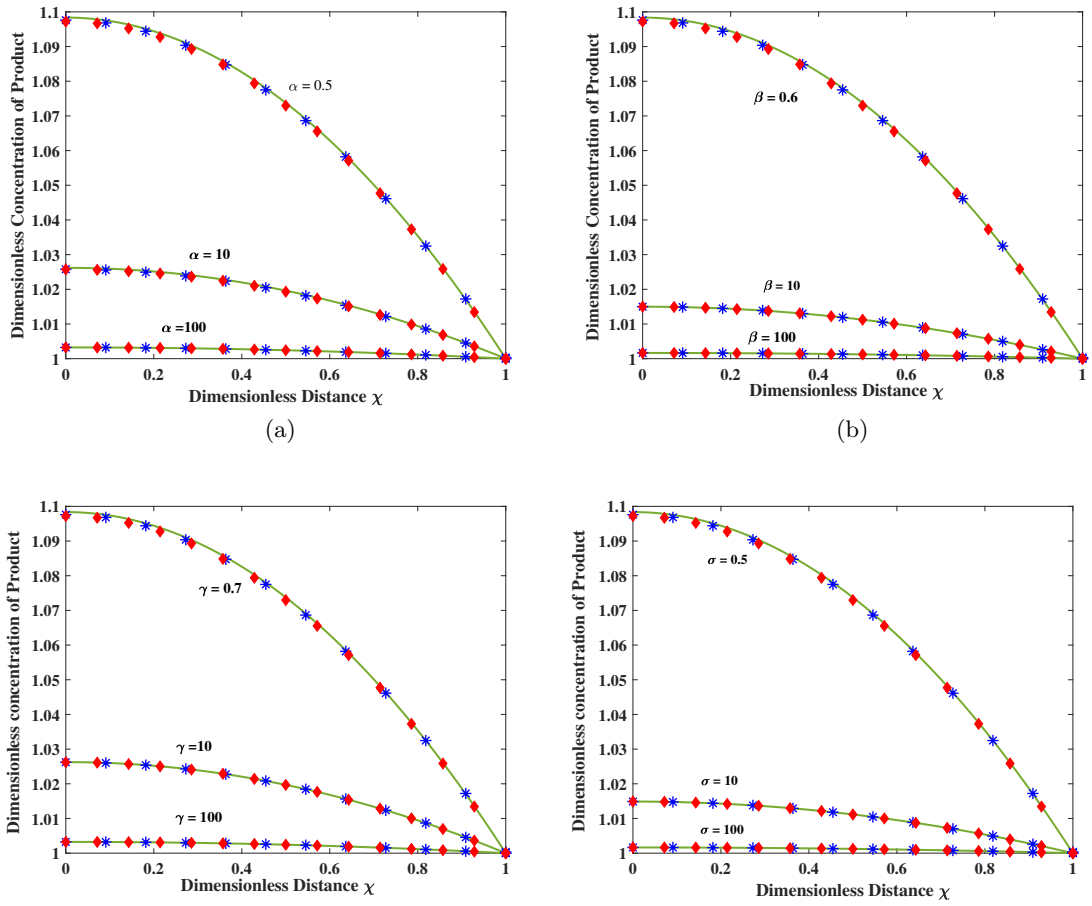

Figure 3: Dimensionless concentration for Product $C(\chi)$ versus the dimensionless distance χ for various values of parameters (3a) α, (3b) β, (3c) γ, (3d) σ where '$\cdots$' denotes the numerical solution, '***' represents the ADM solution, and '$\diamond\diamond\diamond$' corresponds to the TSM solution.

Table 1: Comparison of numerical simulation for the concentration of lactose $A(\chi)$ with analytical solutions obtained using TSM and ADM for fixed parameter values $\alpha = 0.5$,$\beta = 0.6$, $\gamma = 0.7$, $\sigma = 0.5$, $\phi_2^2 = 0.6$, $\phi_3^2 = 0.7$ and varying the ϕ_1^2.

	$\phi_1^2 = 0.1$					$\phi_1^2 = 0.5$					$\phi_1^2 = 1$				
χ	Numerical	TSM	error %	ADM	error%	Numerical	TSM	error %	ADM	error%	Numerical	TSM	error%	ADM	error%
0.0	0.99900	0.99900	0.00000	0.99900	0.00000	0.97590	0.97570	0.02049	0.97560	0.03074	0.90360	0.90460	0.11067	0.90330	0.03320
0.2	0.99904	0.99904	0.00007	0.99904	0.00004	0.97687	0.97667	0.02012	0.97659	0.02852	0.90743	0.90837	0.10410	0.90730	0.01443
0.4	0.99916	0.99916	0.00025	0.99916	0.00016	0.97976	0.97958	0.01879	0.97955	0.02175	0.91893	0.91971	0.08507	0.91930	0.04039
0.6	0.99936	0.99935	0.00054	0.99935	0.00034	0.98458	0.98443	0.01587	0.98448	0.01011	0.93815	0.93868	0.05663	0.93934	0.12714
0.8	0.99963	0.99963	0.00087	0.99963	0.00053	0.99133	0.99123	0.01026	0.99140	0.00695	0.96516	0.96539	0.02411	0.96747	0.23992
1.0	0.99999	0.99998	0.00118	0.99998	0.00067	1.00000	1.00000	0.00038	1.00030	0.03028	1.00005	1.00000	0.00519	1.00377	0.37234
			0.00049		0.00029			0.01432		0.00898			0.06257		0.12203

Table 2: Comparison of numerical simulation for the concentration of oxygen $B(\chi)$ with analytical solutions obtained using TSM and ADM for fixed parameter values $\alpha = 0.5$,$\beta = 0.6$, $\gamma = 0.7$, $\sigma = 0.5$, $\phi_1^2 = 0.5$, $\phi_3^2 = 0.7$ and varying the ϕ_2^2

	$\phi_2^2 = 0.1$					$\phi_2^2 = 0.5$					$\phi_2^2 = 1$				
χ	Numerical	TSM	error %	ADM	error%	Numerical	TSM	error %	ADM	error%	Numerical	TSM	error%	ADM	error%
0.0	1.00100	1.00100	0.00000	1.00100	0.00000	1.02400	1.02400	0.00000	1.02400	0.00000	0.97590	0.97570	0.02049	0.97560	0.03074
0.2	1.00096	1.00096	0.00001	1.00096	0.00001	1.02302	1.02303	0.00066	1.02303	0.00009	0.97590	0.97570	0.02049	0.97560	0.03074
0.4	1.00084	1.00084	0.00005	1.00084	0.00003	1.02010	1.02012	0.00256	1.02010	0.00052	0.97590	0.97570	0.02049	0.97560	0.03074
0.6	1.00065	1.00065	0.00011	1.00065	0.00003	1.01522	1.01527	0.00544	1.01524	0.00178	0.97590	0.97570	0.02049	0.97560	0.03074
0.8	1.00038	1.00038	0.00018	1.00038	0.00002	1.00838	1.00847	0.00885	1.00843	0.00470	0.97590	0.97570	0.02049	0.97560	0.03074
1.0	1.00003	1.00003	0.00025	1.00003	0.00019	0.99958	0.99970	0.01214	0.99968	0.01044	0.97590	0.97570	0.02049	0.97560	0.03074
			0.00010		0.00003			0.00494		0.00292			0.02049		0.03074

Table 3: Comparison of numerical simulation for the concentration of product $C(\chi)$ with analytical solutions obtained using TSM and ADM for fixed parameter values $\alpha = 0.5, \beta = 0.6$, $\gamma = 0.7$, $\sigma = 0.5$, $\phi_1^2 = 0.5$, $\phi_2^2 = 0.6$ and varying the ϕ_3^2

	$\phi_3^2 = 0.3$					$\phi_3^2 = 0.5$					$\phi_3^2 = 0.7$				
χ	Numerical	TSM	error %	ADM	error%	Numerical	TSM	error %	ADM	error%	Numerical	TSM	error%	ADM	error%
0.0	0.99560	0.99560	0.00000	1.00000	0.00000	0.98770	0.98780	0.01012	0.98780	0.01012	1.02400	1.02400	0.00000	1.02400	0.00000
0.2	0.99578	0.99578	0.00022	1.00000	0.00000	0.98819	0.98829	0.00946	0.98829	-0.01017	1.02302	1.02303	0.00066	1.02303	0.00009
0.4	0.99631	0.99630	0.00089	1.00001	0.00000	0.98967	0.98974	0.00740	0.98977	0.01036	1.02010	1.02012	0.00256	1.02010	0.00052
0.6	0.99719	0.99718	0.00193	1.00001	0.00000	0.99213	0.99217	0.00427	0.99224	0.01089	1.01522	1.01527	-0.00544	1.01524	0.00178
0.8	0.99843	0.99840	0.00314	1.00002	0.00000	0.99557	0.99558	0.00061	0.99569	0.01206	1.00838	1.00847	0.00885	1.00843	0.00470
1.0	1.00003	0.99998	0.00429	1.00004	0.00000	1.00000	0.99997	0.00282	1.00014	0.01435	0.99958	0.99970	0.01214	0.99968	-0.01044
			0.00174		0.00000			0.00484		0.01133			0.00494		0.00292

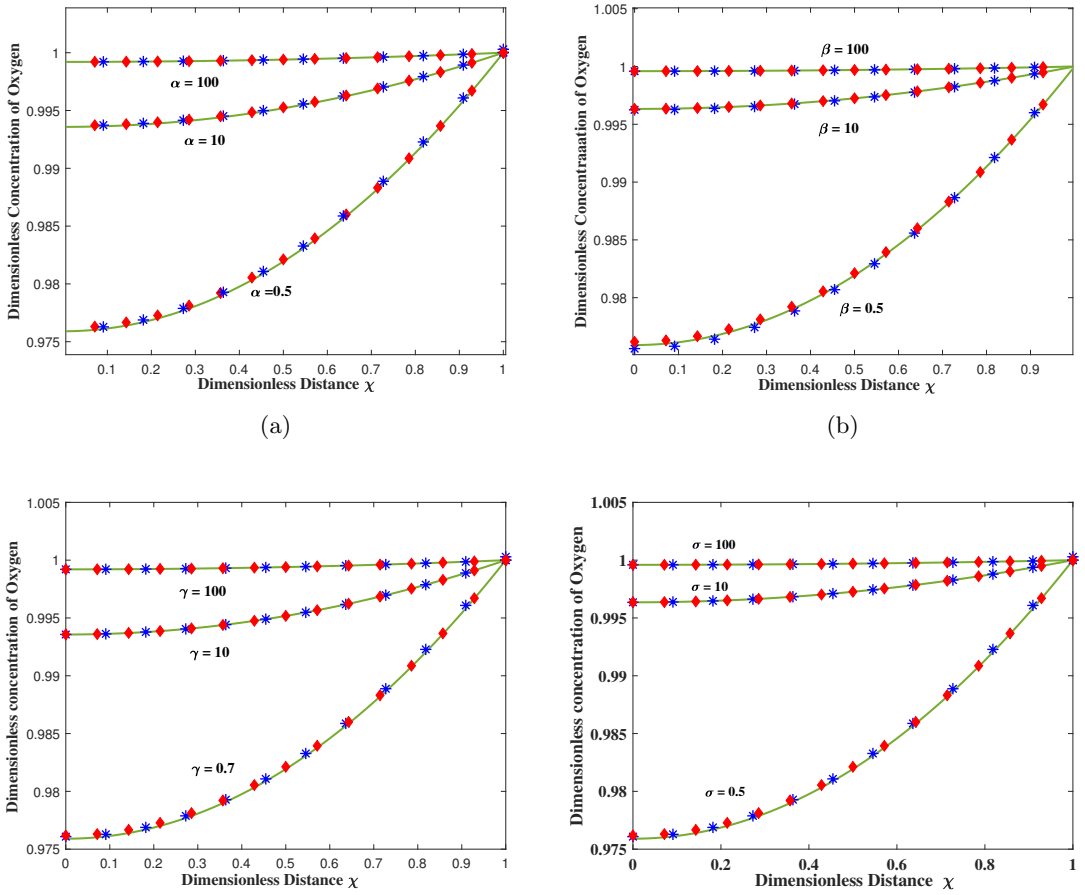

Figure 4: Dimensionless concentration for Oxygen $B(\chi)$ versus the dimensionless distance χ for various values of parameters (4a) α, (4b) β, (4c) γ, (4d) σ where '$\cdots$' denotes the numerical solution, '***' represents the ADM solution, and '$\diamond\diamond\diamond$' corresponds to the TSM solution.

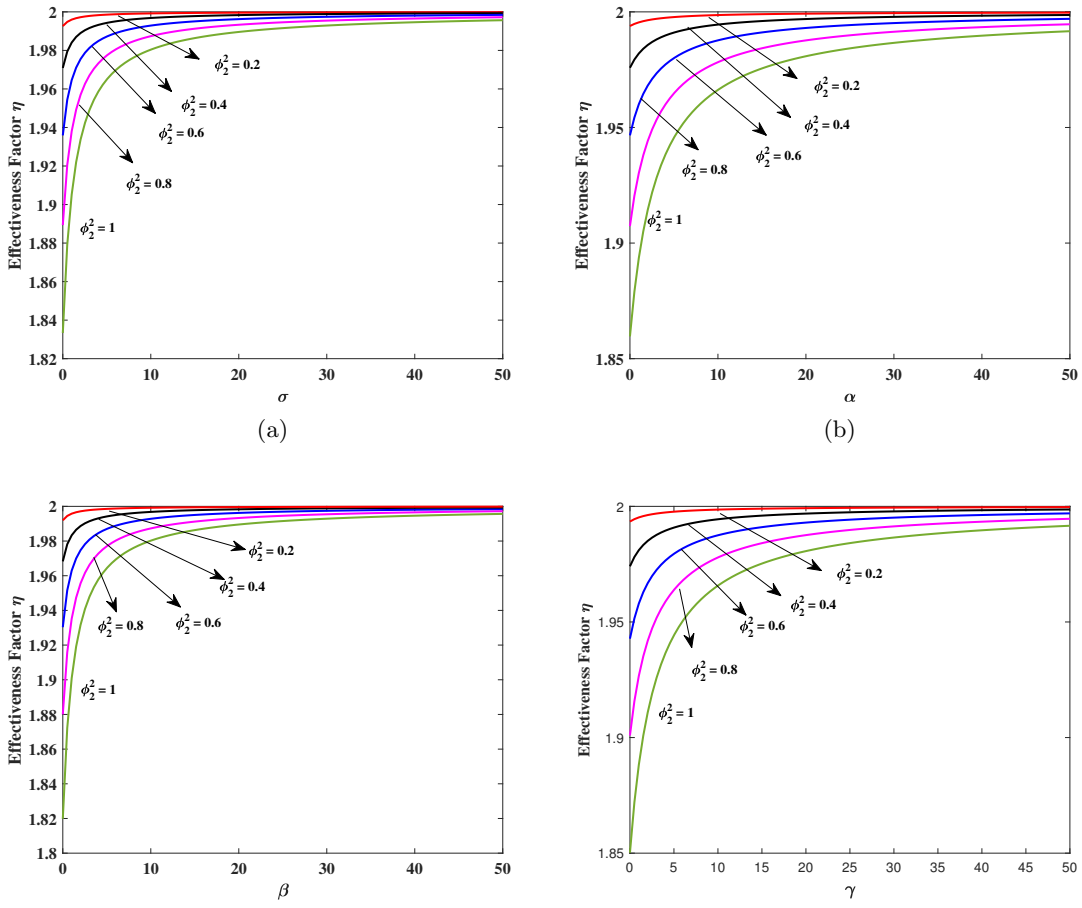

Figure 5: Effectiveness factor versus saturation parameters (5a) σ, (5b) α, (5c) β, (5d) γ for various values of diffusion parameter ϕ_2^2

6. Conclusion

The mathematical model of the carbohydrate oxidation by oxygen catalyzed by the bienzyme glucose dehydrogenase/laccase system immobilized into MR with carbon nanotubes is analyzed by utilizing the semi-analytical methods, namely TSM and ADM. When compared with the numerical simulation, satisfactory results are obtained. The obtained semi-analytical solutions are used to analyze the effects of diffusion and saturation parameters on the concentrations and effective working of the batch reactor. It is observed that the diffusion parameter ϕ_2^2 has the major effect on the working of the batch reactor. As the increase in the diffusion parameter increases, the effectiveness factor of the batch reactor increases.

The proposed theoretical model for the oxidation of carbohydrates by oxygen, catalyzed by the bienzyme glucose dehydrogenase/lactase system immobilized within an MR incorporating carbon nanotubes, offers significant utility for experimental researchers. This model aids in optimizing batch reactor design by evaluating enzyme catalytic loading and particle size, providing a valuable tool for analyzing reaction conditions.

To extend the present mathematical model of carbohydrate oxidation process catalyzed by the glucose dehydrogenase/laccase bienzyme system within a carbon nanotube-based micro-reactor, future work can focus on the development of time-dependent non-steady-state model of the micro-reactor system. This model would enable a deeper understanding of the transient dynamics associated with substrate consumption and product formation, especially during initial stages or under varying input conditions. Further more this model can be extended to the multi-dimensional spatial models for more accurate representation of the porous micro-environment with spherical micro-bioreactors.

A. Semi-analytical expressions utilizing Taylor Series Method

The solution for the governing, Eqs. (12) - (14), for concentration using TSM is expressed as follows:

Considering the series solution for lactose around $\chi = 0$, we have:

$$A(\chi) = \sum_{i=0}^{\infty} \left.\frac{d^i A}{d\chi^i}\right|_{\chi=1} \tag{26}$$

$$= A(1) + \left.\frac{\chi-1}{1!}\frac{dA}{d\chi}\right|_{\chi=1} + \left.\frac{(\chi-1)^2}{2!}\frac{d^2A}{d\chi^2}\right|_{\chi=1} + \left.\frac{(\chi-1)^3}{3!}\frac{d^3A}{d\chi^3}\right|_{\chi=1} + \cdots \tag{27}$$

considering the substrate at $\chi = 1$

$$A(\chi)|_{\chi=1} = 1 \tag{28}$$

$$\left.\frac{dA}{d\chi}\right|_{\chi=1} = l \tag{29}$$

$$\left.\frac{d^2A}{d\chi^2}\right|_{\chi=1} = -2l + \frac{2\phi_1^2}{\alpha + 2\beta + \gamma + 2\sigma} \tag{30}$$

$$\left.\frac{d^3A}{d\chi^3}\right|_{\chi=1} = \frac{\left(\begin{array}{l}\left(6\alpha^2 + (24\beta + 12\gamma + 24\sigma)\alpha + 24\beta^2 + (4\phi_1^2 + 24\gamma + 48\sigma)\beta + \right.\\ \left.6(\gamma + 2\sigma)^2\right) l + 2\phi_1^2\left((n-2)\alpha - 4\beta - 2\gamma - 4\sigma\right)\end{array}\right)}{(\alpha + 2\beta + \gamma + 2\sigma)^2} \tag{31}$$

$$\left.\frac{d^4A}{d\chi^4}\right|_{\chi=1} = \frac{\left(\begin{array}{l} -8(\gamma+2\sigma+\alpha)\beta\phi_1^2 l^2 + \left(16\beta\left((n-1)\alpha-2\beta-\gamma-2\sigma\right)\phi_1^2\right. \\ \left.-192\left(\frac{\gamma}{2}+\sigma+\frac{\alpha}{2}+\beta\right)^3\right) l - 8\phi_1^2\left(-\beta\phi_1^2+(n-2)\alpha^2+\right. \\ \left.\left((n^2+2n-8)\beta+\left(\frac{n^2}{2}+n-4\right)\gamma+(n^2+2n-8)\sigma-\frac{\phi_3^2}{4}\right)\alpha\right. \\ \left.-8\left(\frac{\gamma}{2}+\sigma+\beta\right)^2\right) \end{array}\right)}{(\alpha+2\beta+\gamma+2\sigma)^3} \tag{32}$$

$$\left.\frac{d^5A}{d\chi^5}\right|_{\chi=1} = \frac{\left(\begin{array}{l} 16\beta\left(\left(-3l+\frac{7n}{2}-2\right)\alpha+(l-4)\beta-3\left(l+\frac{2}{3}\right)(\gamma+2\sigma)\right)\phi_1^4 \\ +\left((40n-80)\alpha^3+\left((24l^3+(-48n+64)l^2+(24n^2-128n+80)l\right.\right. \\ \left.+64n^2+160n-480)\beta+(32n^2+80n-240)\gamma+(64n^2+160n-480)\sigma\right. \\ \left.+2\phi_3^2(n-4)\right)\alpha^2+\left(((48n+128)l^2+(-96n^2-256n+320)l+48n^3\right. \\ \left.+128n^2+160n-960)\beta^2+\left((48\gamma+96\sigma)l^3-48(n-\frac{8}{3})(\gamma+2\sigma)l^2\right.\right. \\ \left.+\left((-48n^2-128n+160)\gamma+(-96n^2-256n+320)\sigma+28\phi_3^2\right)l\right. \\ \left.+(48n^3+128n^2+160n-960)\gamma+(96n^3+256n^2+320n-1920)\sigma\right. \\ \left.-24\phi_3^2(n+\frac{2}{3})\right)\beta+12\left((n^3+\frac{8}{3}n^2+\frac{10}{3}n-20)\gamma+\left(2n^3+\frac{16}{3}n^2+\frac{20}{3}n\right.\right. \\ \left.\left.-40\right)\sigma-\phi_3^2(n+\frac{2}{3})\right)(\gamma+2\sigma)\right)\alpha+(320l-640)\beta^3+128\left(l^2+\frac{5}{2}l-\frac{15}{2}\right) \\ (\gamma+2\sigma)\beta^2+24(l^3+\frac{8}{3}l^2+\frac{10}{3}l-20)(\gamma+2\sigma)^2\beta-80(\gamma+2\sigma)^3\Big)\phi_1^2 \\ +1920\left(\frac{\gamma}{2}+\sigma+\frac{\alpha}{2}+\beta\right)^4 l \end{array}\right)}{(\alpha+2\beta+\gamma+2\sigma)^4} \tag{33}$$

using the Eqs. (28) - (33) we get the solution of the lactose concentration as given in (18). By following the same methodology we can find the semi-analytical solutions of product $B(\chi)$ and oxygen $C(\chi)$ concentrations.

B. Semi-analytical expressions utilizing Adomian Decomposition Method

The non linear governing Eqs. (12) - (14) are solved using the ADM, by applying

$$L[A(\chi)] = \phi_1^2 N[A(\chi), C(\chi), B(\chi)], \tag{34}$$

$$L[C(\chi)] = -\phi_2^2 N[A(\chi), C(\chi), B(\chi)], \tag{35}$$

$$L[B(\chi)] = \frac{\phi_3^2}{2} N[A(\chi), C(\chi), B(\chi)], \tag{36}$$

where

$$L = \frac{d^2}{d\chi^2},$$

$$L^{-1}(.) = \int\int (.)\, d\chi d\chi,$$

$$N[A(\chi)] = -\frac{2}{\chi}\frac{dA(\chi)}{d\chi} = \phi_1^2 \frac{2A(\chi)B(\chi)}{\alpha A(\chi) + 2\beta B(\chi) + \gamma A(\chi)B(\chi) + 2\sigma A(\chi)B(\chi)}, \tag{37}$$

utilizing the inverse operator in Eqs. (34) - (36)

$$A(\chi) = D_1\chi + D_2 + \phi_1^2 L^{-1} N[A(\chi)], \tag{38}$$

$$C(\chi) = D_3\chi + D_4 + \phi_2^2 L^{-1} N[C(\chi)], \tag{39}$$

$$B(\chi) = D_5\chi + D_6 + \phi_3^2 L^{-1} N[B(\chi)], \tag{40}$$

where D_1, D_2, D_3, D_4, D_5, and D_6 are integration constants.
The ADM assumes an infinite series solution for the unknown functions $A(x)$, $B(x)$, $C(x)$ of Eqs. (34)–(36), given by [32–34] as follows:

$$A(x) = \sum_{n=0}^{\infty} A_n(x), \tag{41}$$

$$C(x) = \sum_{n=0}^{\infty} C_n(x), \tag{42}$$

$$B(x) = \sum_{n=0}^{\infty} B_n(x), \tag{43}$$

and decomposing the non-linear operator N as

$$N[A(x)] = \sum_{n=0}^{\infty} F_n(x), \tag{44}$$

F_n are called Adomian polynomials of $A_0, A_1, \ldots, A_n$ [33, 34] and are formed by

$$F_n(x) = \frac{1}{n!}\frac{d^n}{d\lambda^n}\left[N\left(\sum_{i=0}^{\infty}\lambda_i A_i(x)\right)\right]\Bigg|_{\lambda=0}, \quad n = 0, 1, 2, \ldots \tag{45}$$

Substituting Eqs. (41)–(45) into Eqs. (38)–(40), we get the following iterations:

$$A_1 = 1 \qquad\qquad A_0' = 0 \tag{46}$$

$$A_{n+1} = D_2 + \phi_1^2 L^{-1} N[A(\chi)] = D_2 + \phi_1^2 L^{-1} F_n(\chi), \quad n \geq 0 \tag{47}$$

Similarly for,

$$C_{n+1} = D_4 + \phi_2^2 L^{-1} N[B(\chi)] = D_4 + \phi_2^2 L^{-1} F_n(\chi), \quad n \geq 0 \tag{48}$$

$$B_{n+1} = D_6 + \phi_3^2 L^{-1} N[C(\chi)] = D_6 + \phi_3^2 L^{-1} F_n(\chi), \quad n \geq 0 \tag{49}$$

$$F_0(\chi) = N[A(\chi)] = \frac{A_0 B_0}{\alpha A_0 + 2\beta B_0 + \gamma A_0 B_0 + \sigma A_0 B_0} = \frac{1}{3(\alpha + 2\beta + \gamma + 2\sigma)}, \tag{50}$$

using Eqs. (47) - (49) we get

$$\begin{aligned} A_1(\chi) &= D_2 + \phi_1^2 L^{-1} F_0(\chi) = D_2 + \phi_1^2 L^{-1} \left(\frac{1}{3(\alpha + 2\beta + \gamma + 2\sigma)} \right), \\ &= \frac{\phi_1^2(\chi^2 - 1)}{3(\alpha + 2\beta + \gamma + 2\sigma)} \end{aligned} \tag{51}$$

Similarly for

$$\begin{aligned} C_1(\chi) &= D_4 + \phi_2^2 L^{-1} F_0(\chi) = D_4 + \phi_2^2 L^{-1} \left(\frac{1}{3(\alpha + 2\beta + \gamma + 2\sigma)} \right), \\ &= \frac{\phi_2^2(1 - \chi^2)}{3(\alpha + 2\beta + \gamma + 2\sigma)}, \end{aligned} \tag{52}$$

$$\begin{aligned} B_1(\chi) &= D_6 + \phi_3^2 L^{-1} F_0(\chi) = D_6 + \phi_3^2 L^{-1} \left(\frac{1}{3(\alpha + 2\beta + \gamma + 2\sigma)} \right), \\ &= \frac{\phi_3^2(\chi^2 - 1)}{6(\alpha + 2\beta + \gamma + 2\sigma)}, \end{aligned} \tag{53}$$

Then $F_1(\chi)$ can be obtained by following boundary conditions

$$A_1(0) = 0, \qquad A_1(1) = 1 \tag{54}$$

$$F_1(\chi) = \frac{d}{d\lambda} \left(N[A_0 + \lambda A_1] \right)_{\lambda=0}$$

and

$$A_i'(0) = 0, \quad A_i(1) = 0, \quad i \geq 0 \tag{55}$$

$$\begin{aligned} A_2(\chi) &= D_2 + \phi_1^2 L^{-1} F_0(\chi), \\ &= D_2 + \phi_1^2 L^{-1} \left(\frac{(\chi^2 - 1)(\alpha\phi_3^2 + 4\beta\phi_1^2)}{,} 6(\alpha + \gamma + 2\beta + 2\sigma)^3 \right) \\ A_2(\chi) &= \phi_1^2 \frac{(\chi^2 - 1)(\alpha\phi_3^2 + 4\beta\phi_1^2)}{6(\alpha + \gamma + 2\beta + 2\sigma)^3} \left(\frac{\chi^4}{20} - \frac{\chi^2}{6} + \frac{7}{60} \right), \end{aligned} \tag{56}$$

the concentration of lactose $A(\chi)$ is determined by summing Eqs. (46), (53), and (56). Using a similar approach, the solutions for the concentration of the product $C(\chi)$ and the concentration of oxygen $B(\chi)$ can also be obtained.

Acknowledgements

The authors are very much thankful to the management, SRM Institute of Science and Technology for their continuous support and encouragement.

Author Contributions

Daniel S; Data curation, Writing-original draft, Formal analysis, Methodology, Software, Visualization. **Mallikarjuna M**; Data curation, Writing-original draft, Formal analysis, Methodology, Software, Visualization. **Senthamarai R**; Formal analysis, Methodology, Validation, Resources, Writing review and editing and Supervision.

Declarations

Funding This research did not receive any specific grant from funding agencies in the public, commercial, or not-for-profit sectors.

Conflict of interest The authors declare that they have no conflict of interest.

References

[1] J. Iqbal, S. Iqbal, and C. E. Müller. Advances in immobilized enzyme microbioreactors in capillary electrophoresis. *Analyst*, 138(11):3104–3116, 2013.

[2] D. Schäpper, M. N. H. Z Alam, N. Szita, A. Eliasson Lantz, and K. V Gernaey. Application of microbioreactors in fermentation process development: a review. *Analytical and bioanalytical chemistry*, 395:679–695, 2009.

[3] G. Maria. Enzymatic reactor selection and derivation of the optimal operation policy, by using a model-based modular simulation platform. *Computers & chemical engineering*, 36:325–341, 2012.

[4] E. Papadakis, S. Pedersen, A. K. Tula, M. Fedorova, M. J. Woodley, and R. Gani. Model-based design and analysis of glucose isomerization process operation. *Computers & Chemical Engineering*, 98:128–142, 2017.

[5] W. Tischer and F. Wedekind. Immobilized enzymes: methods and applications. *Biocatalysis-from discovery to application*, pages 95–126, 1999.

[6] A. Y. Khan, S. B. Noronha, and R. Bandyopadhyaya. Glucose oxidase enzyme immobilized porous silica for improved performance of a glucose biosensor. *Biochemical engineering journal*, 91:78–85, 2014.

[7] L. T. Zhu, W. Y. Ma, and Z. H. Luo. Influence of distributed pore size and porosity on mto catalyst particle performance: Modeling and simulation. *Chemical Engineering Research and Design*, 137:141–153, 2018.

[8] P. M. Doran. *Bioprocess engineering principles*. Elsevier, 1995.

[9] J. Villadsen. Principles of metabolic engineering. *Biotechnology*, 3:226–256, 2009.

[10] M. Al-Shannag, Z. Al-Qodah, J. Herrero, A. J. Humphrey, and F. Giralt. Using a wall-driven flow to reduce the external mass-transfer resistance of a bio-reaction system. *Biochemical engineering journal*, 39(3):554–565, 2008.

[11] R. Baronas, J. Kulys, and L. Petkevičius. Modeling carbohydrates oxidation by oxygen catalyzed by bienzyme glucose dehydrogenase/laccase system immobilized into

microreactor with carbon nanotubes. *Journal of Mathematical Chemistry*, 59:168–185, 2021.

[12] J. B. Sánchez, M. Vuono, and D. Dionisi. Model-based comparison of sequencing batch reactors and continuous-flow activated sludge processes for biological wastewater treatment. *Computers & Chemical Engineering*, 144:107127, 2021.

[13] F. F. Rivera, T. Pérez, L. F. Castañeda, and J. L. Nava. Mathematical modeling and simulation of electrochemical reactors: A critical review. *Chemical engineering science*, 239:116622, 2021.

[14] O. Harker-Sanchez, A. A. Jaramillo, and D. M. Arias. Method to obtain parameters k2, k3 for dilution rate observer in am2 model of the anaerobic digestion process in a batch reactor. *Energy Sources, Part A: Recovery, Utilization, and Environmental Effects*, 46(1):3110–3123, 2024.

[15] M. Mallikarjuna and R. Senthamarai. An amperometric biosensor and its steady state current in the case of substrate and product inhibition: Taylors series method and adomian decomposition method. *Journal of Electroanalytical Chemistry*, 946:117699, 2023.

[16] M. Mallikarjuna, J. L. G. Guiraob, and R. Senthamarai. Theoretical analysis of amperometric biosensor with substrate and product inhibition involving non-michaelis-menten kinetics. *MATCH Communications in Mathematical and Computer Chemistry*, 93:319–347, 2025.

[17] M. Mallikarjuna and R. Senthamarai. Mathematical analysis of batch reactor performance for the enzymatic synthesis of cephalexin: Laplace homotopy perturbation method and adomian decomposition method. *Partial Differential Equations in Applied Mathematics*, 11:100806, 2024.

[18] M. Sivakumar, M. Mallikarjuna, and R. Senthamarai. A kinetic non-steady-state analysis of immobilized enzyme systems without external mass transfer resistance. *International Journal of Analysis and Applications*, 22:31–31, 2024.

[19] M. Sivakumar, M. Mallikarjuna, and R. Senthamarai. A kinetic non-steady state analysis of immobilized enzyme systems with external mass transfer resistance. *AIMS Mathematics*, 9(7):18083–18102, 2024.

[20] W. Al-Hayani. Combined laplace transform-homotopy perturbation method for sine-gordon equation. *Applied Mathematics & Information Sciences*, 10:1781–1786, 2016.

[21] R. Senthamarai and T. N. Saibavani. Substrate mass transfer: analytical approach for immobilized enzyme reactions. In *Journal of Physics: Conference Series*, volume 1000, page 012146. IOP Publishing, 2018.

[22] W. M. Al-Hayani and M. T. Younis. Solving fuzzy system of boundary value problems by homotopy perturbation method with green's function. *European Journal of Pure and Applied Mathematics*, 16(2):1236–1259, 2023.

[23] W. M. Al-Hayani and M. T. Younis. The homotopy perturbation method for solving nonlocal initial-boundary value problems for parabolic and hyperbolic partial differential equations. *European Journal of Pure and Applied Mathematics*, 16(3):1552–1567, 2023.

[24] A. El-Ajou, H. Al-ghananeem, R. Saadeh, A. Qazza, and M. A. N. Oqielat. A modern

analytic method to solve singular and non-singular linear and non-linear differential equations. *Frontiers in Physics*, 11:1167797, 2023.

[25] M. O. Olayiwola, A. I. Alaje, A. O. Yunus, K. A. Adedokun, and K. A. Bashiru. A mathematical modeling of covid-19 treatment strategies utilizing the laplace adomian decomposition method. *Results in Control and Optimization*, 14:100384, 2024.

[26] R. O. Awonusika. Analytical solution of a class of lane–emden equations: Adomian decomposition method. *The Journal of Analysis*, 32(2):1009–1056, 2024.

[27] A. S. Mahmood, L. Casasús, and W. Al-Hayani. Analysis of resonant oscillators with the adomian decomposition method. *Physics Letters A*, 357(4-5):306–313, 2006.

[28] W. Al-Hayani. Adomian decomposition method with green's function for solving twelfth-order boundary value problems. *Applied Mathematical Sciences*, 9:353–368, 01 2015.

[29] M. Usman, H. U. Khan, M. Sarwar, N. Fatima, and K. Abodayeh. An innovative analytical result of two-dimensional heat equation using joint mechanism of natural transform and adomian decomposition method. *European Journal of Pure and Applied Mathematics*, 18(2):6051–6051, 2025.

[30] V. Silambuselvi, P. Jeyabarathi, N. Jha, K. Angaleeswari, T. R. K. Kumar, and L. Rajendran. Theoretical analysis of facilitated diffusion process in a liquid membrane: Adomian decomposition method. *International Journal of Electrochemical Science*, 19(12):100855, 2024.

[31] B. Mebarek, A. Maatoug, S. A. M. Mostefaoui, H. Benali, and Y. El Guerri. Adomian decomposition method for modelling the growthof feb/fe2b layer in boronizing process. *Zastita Materijala*, 66(1):148–157, 2025.

[32] G. Adomian. *Nonlinear stochastic operator equations*. Academic press, 1986.

[33] G. Adomian. *Nonlinear stochastic systems theory and applications to physics*, volume 46. Springer Science & Business Media, 1988.

[34] G. Adomian. *Solving frontier problems of physics: the decomposition method*. Springer Science & Business Media, 1994.